where α is an auxiliary variable introduced for convenience of calculation. Putting $\alpha s=y$, we get

$$D=\int_0^2 d^3s\,\frac{4\pi^2}{s}\int_0^\infty e^{-sy}\left[\frac{1}{y^3}\{sye^{(-s/2)y}+e^{-y}(y+1)(e^{-sy}-1)\}\right]^2 dy+\int_0^\infty d^3s\,\frac{4\pi^2}{s}\int_0^\infty e^{-sy}\left[\frac{1}{y^3}\{e^y(y-1)+e^{-y}(y+1)\}\right]^2 dy. \quad \text{(A2)}$$

The integration with respect to y is elementary but tedious. After integration we put $s=2u$ and obtain the following results:

$$D=\frac{64}{15}\pi^3\int_0^\infty P(u)du. \quad \text{(A3)}$$

For $u<1$,

$$\begin{aligned}P(u)&=P_1(u)\\&=[4+(15/2)u-5u^3+\tfrac{3}{2}u^5]\ln(1+u)+29u^2+3u^4\\&\quad+[4-(15/2)u+5u^3-\tfrac{3}{2}u^5]\\&\quad\times\ln(1-u)-40u^2\ln 2\\&\cong 40(1-\ln 2)u^2-10u^4+\tfrac{4}{3}u^6+0.21u^8. \quad \text{(A4)}\end{aligned}$$

For $u>1$,

$$\begin{aligned}P(u)&=P_2(u)\\&=[4-20u^2-20u^3+4u^5]\ln(u+1)+4u^3+22u\\&\quad+[-4+20u^2-20u^3+4u^5]\ln(u-1)\\&\quad+(40u^3-8u^5)\ln u\cong\frac{10}{3}\frac{1}{u}+\frac{1}{3}\frac{1}{u^3}+0.16\frac{1}{u^5}. \quad \text{(A5)}\end{aligned}$$

The error of the above power-series expansions is less than 0.1% for $P_1(u)$ and less than 0.5% for $P_2(u)$.

PHYSICAL REVIEW VOLUME 116, NUMBER 2 OCTOBER 15, 1959

Heavy Nuclei in the Primary Cosmic Radiation at Prince Albert, Canada. I. Carbon, Nitrogen, and Oxygen*

H. Aizu,† Y. Fujimoto, S. Hasegawa, M. Koshiba, I. Mito,‡ J. Nishimura, K. Yokoi,‡
Institute for Nuclear Study, University of Tanashi, Tokyo, Japan

AND

Marcel Schein, *Enrico Fermi Institute for Nuclear Studies, Department of Physics, University of Chicago, Chicago, Illinois*

(Received May 22, 1959)

A stack of G-5 emulsion, exposed at 120 000 feet for 8 hours at 61°N has been used to study the charge and energy spectrum of heavy nuclei at the low-energy end. Energy measurements have been made on C, N, and O nuclei up to 1 Bev/nucleon. The spectrum shows a broad maximum at 550 Mev/nucleon, extrapolated to the top of the atmosphere. Various possibilities to explain this spectrum are discussed. However, it seems desirable to determine the energy spectrum of the other heavy-nuclei components in this energy region in order to gain a more complete understanding of the whole problem. Measurements of this kind are in progress and will be reported.

1. INTRODUCTION

In order to gain information concerning the acceleration mechanism of the primary radiation, the study of the heavy-nuclei component in the cosmic radiation has certain advantages over studies on primary protons and the various secondary components. This is due to the fact that heavier nuclei cannot be created from lighter elements once they are ejected from the source into interstellar space. Any conceivable process the primary cosmic radiation might undergo in interstellar space takes place in the direction from heavier to lighter elements.

The very existence of the heavy-nuclei component[1] poses stringent restrictions on the possible types of acceleration mechanisms. Furthermore, the determination of the fluxes of Li, Be, and B [2] has so far been the only method of estimating the average age of the primary cosmic radiation.

The study of the heavier Z components can yield valuable information regarding the relative abundances

* This work has been supported in part by the U. S. National Committee of IGY, the National Science Foundation, and the joint program of the Office of Naval Research and the U. S. Atomic Energy Commission.

† Department of Physics, Rikkyo University, Tokyo, Japan.
‡ College of General Education, University of Tokyo, Tokyo, Japan.

[1] Freier, Ney, and Oppenheimer, Phys. Rev. **75**, 991 (1949). H. L. Bradt and B. Peters, Phys. Rev. **77**, 54 (1950); **80**, 943 (1950).

[2] Koshiba, Schultz, and Schein, Nuovo cimento **9**, 1 (1958).

of medium and heavy elements.[2] Certain types of stars were suggested by Koshiba, Schultz, and Schein[2] as possible primary sources of the cosmic radiation.

However, while our experimental data concerning heavy nuclei in the latitude-dependent rigidity region, say from 3 Bev/c to 15 Bev/c, is probably correct, we have practically no data at the low-rigidity end, except on α-particles studied by the Minnesota and Bristol groups.[3] Recalling the two characteristic features of heavy nuclei, i.e., their fragile structure which can easily be destroyed in interactions at cosmic-ray energies and their appreciable ionization in passing through matter, one can easily see the kind of information we can obtain in this field. The effect of ionization loss will be most pronounced at the low-energy end of the spectrum. Though we know qualitatively that the ionization loss represents a serious difficulty in the original version of Fermi's theory of the acceleration mechanism, we do not know quantitatively how important this process is in building up the cosmic radiation.

In view of the above considerations, an investigation of the low-rigidity heavy-nuclei component of the primary cosmic radiation was undertaken in the summer of 1957 at the University of Chicago by two of the authors (M. S. and M. K.). The requirements set forth for the experiments were as follows: (1) it should cover the rigidity spectrum to as low a value as our present experimental techniques allow us to go; (2) it should yield a clear-cut separation of charges and good energy resolution of heavy nuclei up to an energy of 500 Mev/nucleon at least, and (3) a measurement of the time fluctuation of the heavy component should be attempted. For this purpose, a stack of Ilford G-5 nuclear emulsion and a moving plate mechanism, as shown in Fig. 1 and described in the next section, has been flown at Prince Albert, Canada (61°N geomagnetic latitude) in a Skyhook Balloon and exposed to the primary cosmic radiation. Prince Albert is located north of Minneapolis, which we know is already beyond the knee of the latitude curve for α-particles.[3] The stack was flown for 8 hours at an altitude of 120 000 ft.[4] All plates were processed at the University of Chicago. The preliminary analysis of the stack was carried out at Chicago and continued at the Institute for Nuclear Study, University of Tokyo. The present paper is dealing with the energy spectrum of C, N, and O nuclei and their relative abundance in the primary cosmic radiation. Studies carried out on other nuclei will be published later.

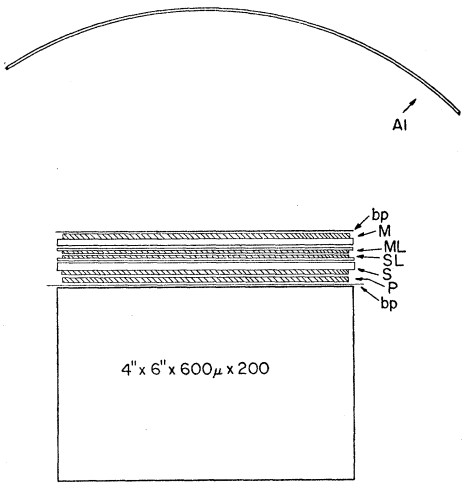

FIG. 1. Schematic drawing of gondola, showing the arrangement of stack and moving-plate mechanism. Al—aluminum sphere $\frac{1}{16}$ in. thick, *bp*—black paper, *M* and *S*—600 μ glass-backed plate, *ML* and *SL*—200 μ Lucite-backed plate, *P*—600 μ pellicle.

2. EXPERIMENTAL PROCEDURES

Two hundred pellicles of Ilford G-5 nuclear emulsions of 4 in.×6 in., 600 μ in thickness, were stacked underneath a moving-plate mechanism[5] consisting of two horizontal Lucite plates, 6 in.×6 in. each, coated with 200 μ thick G-5 emulsion. A glass-backed G-5 emulsion and a pellicle, each 6 in.×6 in. and 600 μ in thickness, were inserted between the stack and the moving-plate mechanism for the purpose of correlating the tracks passing through the whole system. An additional glass-backed G-5 emulsion 6 in.×6 in. and 600 μ in thickness was placed horizontally on the very top of the assembly, its emulsion surface facing upward. The whole assembly was rigidly mounted into a pressurized aluminum sphere. The geometry of the apparatus is shown in Fig. 1. The aluminum sphere was covered by 3 inches of styrofoam in order to avoid excessive heating of the stack during the flight. The exposure took place at Prince Albert (Canada), 61°N geomagnetic latitude, on September 11, 1957. The pressure was measured by an accurate Wallace Tierman gauge, photographed at 3-minute intervals, at higher altitudes, and by a radiosonde type gauge at lower altitudes. The flight curve is plotted in Fig. 2. The pressure in millibars and the height in feet are plotted against the local time, C. S. T.

In order that the entire stack could be processed simultaneously, a wet hot stage with half-strength developer at 25°C for 80 minutes was used. The result was that while the minimum grain density is 23 grains/100 μ, the grain size is of the order of 0.6 micron. Accordingly the gap-density is reduced to 8 gaps/100 μ for relativistic carbon as compared to 30 gaps/100 μ observed previously.[2]

The scanning for C, N, and O nuclei was carried out at the top edge of the stack. The central 10-cm region

[3] Fowler, Waddington, Freier, Naugle, and Ney, Phil. Mag. **2**, 157 (1957); F. B. McDonald, Phys. Rev. **107**, 1386 (1957); Freier, Ney, and Fowler, Nature **4619**, 1321 (1958).

[4] We wish to express our appreciation to the Raven Corporation for launching the balloon and recovering the stack.

[5] J. J. Lord and M. Schein, Phys. Rev. **78**, 484 (1950); V. H. Yngve, Phys. Rev. **92**, 428 (1953); M. Koshiba and M. Schein, Phys. Rev. **103**, 1820 (1956).

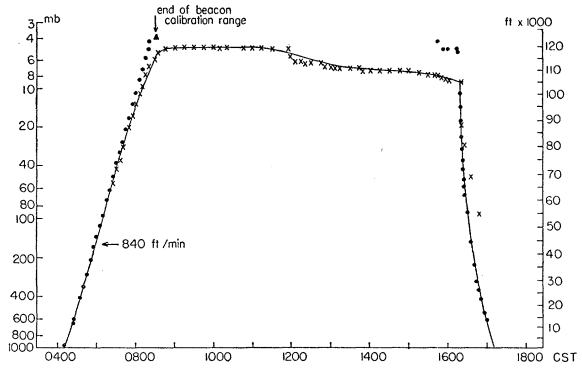

FIG. 2. The flight curve of the exposure. ×: pressure determined from photographing Wallace-Tiernan gauge. o: pressure determined from radio-sonde.

of each plate had been scanned using 10×10 magnification at the top for those tracks which satisfy the following three criteria: (1) the projected zenith angle in the emulsion plane does not exceed 20°, (2) the track length per plate in the zenith direction is larger than or equal to 3 mm, and (3) the ionization is at least that corresponding to a relativistic boron nucleus. The third criterion can easily be applied once a good case of a relativistic carbon breakup into three α's is found, since then the approximate gap density of a relativistic boron track can be obtained from measurements of relativistic carbon and α particles by the use of previous results on gap density.[2] However, the visual inspection is in most cases quite reliable in separating relativistic boron from relativistic beryllium, since there is a considerable difference in appearance between the two. In case there was some ambiguity on whether or not the ionization of the track satisfied the criterion, a gap density of 15 gaps/100 μ or less was required. This, as will be shown later, included some relativistic beryllium too. Hence the tracks of ionization equal to or larger than that of relativistic carbon could not escape being recorded once they were inspected.

Every track located by this method has a potential range in the stack of 10 cm or more. All of these tracks have been traced until they leave the stack at the bottom, stop inside the stack, or interact.

3. DETERMINATION OF CHARGE AND ENERGY

It is well known that in the energy range where the ionization of a heavy nucleus changes considerably with the velocity, charge and energy determination cannot be made separately. We have to make measurements of two independent parameters in order to specify the charge and energy.

To establish a calibration curve for the ionization, we start with the study of tracks which are known to be relativistic from the observed nuclear interaction they produce. The results of the conventional 4-grain δ-ray countings on these tracks are shown in Fig. 3 in the form of a histogram. The counting has been performed by three different observers and the countings on the same track by different observers are counted as different cases. In each case a total of at least 400 δ-rays have been counted. Some of the tracks have been counted by all three observers and the average taken over the countings of the three observers has been used for each track. This is shown in Fig. 3 in the shaded histogram. The cases shown include the fragmentation of one $C \rightarrow 3\alpha$ and one $O \rightarrow 4\alpha$, both at relativistic energies. A clear-cut separation of C, N, O tracks at relativistic energies is observed in Fig. 3.

The gap-counting, or blob-counting, on tracks of C, N, O cannot be expected to compete as favorably with the 4-grain δ-day counting as in the previous work[2] mainly because of the smaller gap-density due to the overdevelopment of the stack. Nevertheless, it was done in order to obtain (1) an accurate gap-density calibration from plate to plate which is a necessity for the analysis of Li, Be, and B; and (2) a checking of the results of the δ-ray countings. The charge assignments of relativistic tracks by the method of gap-counting, calibrated against the $C \rightarrow 3\alpha$ and $O \rightarrow 4\alpha$ cases mentioned above, are found to be in a very good agreement with those of the 4-grain δ-ray countings. The details of the gap-countings will be discussed in the forthcoming paper on Li, Be, and B. We may mention here that the use of stopping particles with identified charge made it possible to obtain an accurate calibration curve for ionization by this method.

Our next problem is of identifying slow particles, and we shall start with those cases where the particles stopped in the stack. The usual methods for determining the charge of stopping heavy-nuclei tracks are as follows: (1) δ-ray density *versus* residual range, (2) the effective track width, (3) the thin-down length, and (4) the variations of the above. In this investigation, method (1) was employed. The ordinary δ-ray counting, of the 4- or 7-grain convention, obviously cannot be used for the stopping C, N, and O nuclei, not only because of too high δ-ray densities, but also because there is a systematic variation of the cutoff energy of

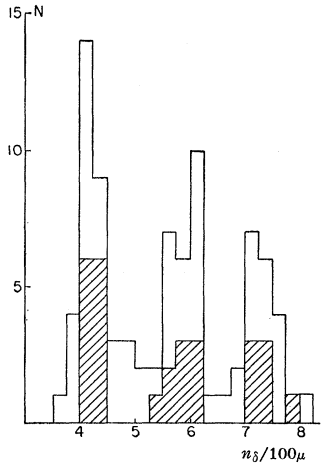

FIG. 3. Distribution of delta-ray densities, n_δ, of high-energy tracks. For details, see text.

δ-rays with varying width of the completely blackened track core. Therefore, a cutoff procedure free from this systematic variation must be employed. We applied a criterion by which we count only those δ-rays which extend beyond a certain distance from the center of the track. After some trial countings, we set this distance to be 4.38 μ. By using this criterium, each stopping track had been δ-ray counted from the end of its range backward over a track length of at least 20 fields of view, i.e., a total length of 2.6 mm. The integrated number of δ-rays counted in this way has a stronger dependence on the charge of the particle than the δ-ray density of a relativistic particle which has the well-known Z^2 dependence, because of the additional $1/Z$ dependence of the residual range for a given velocity. The calibration using this method has been carried out in the following manner: We first counted the δ-rays of stopping α-particles, which are easily recognizable as such when they are several centimeters long, and then plotted the integral number of δ-rays as a function of the residual range.

The δ-ray density n_δ has the form $Z^2f(v)$ while the residual range R is of the form $(M/Z^2)g(v)$ (M is the mass of the nucleus). Hence, the relation between n_δ and R is

$$n_\delta = Z^2h(Z^2R/M),$$

which is the similarity law of the δ-ray density. The integral number of δ-rays, N_δ, as a function of the residual range, becomes

$$N_\delta = \int_0^R n_\delta dR = \int_0^R Z^2h\left(\frac{Z^2}{M}R\right)dR$$

$$= \int_0^{Z^2/RM} Mh\left(\frac{Z^2}{M}R\right)d\left(\frac{Z^2}{M}R\right) = MH\left(\frac{Z^2}{M}R\right).$$

This expresses the similarity law of the integral number of δ-rays of particles of different mass and different charge. For the same value of the mass to charge ratio, the expression reduces to the simpler form

$$N_\delta = ZH'(ZR).$$

The calibration for determining the charge can be obtained by using this similarity law of the integral δ-ray number *versus* residual range for α-particles as shown in Fig. 4(a). The contribution of background electrons is negligible because of the large value of the cutoff used in the δ-ray range (4.38 μ). A correction, however, has to be made for the effect inherent for any method utilizing certain specified portions of a track. Namely, the specified portion may happen to be in an unfavorable part of the emulsion, i.e., in the vicinity of defective spots. The correction for the variation has been made by using high-energy tracks of appropriate charge range, $Z\sim 14$. The results, after this correction has been applied, are shown in Fig. 4(b), where the stopping particles are classified according to the number of δ-rays on the last 2.6 mm of their residual ranges. One can clearly see in the figure the separation of C, N, and O nuclei.

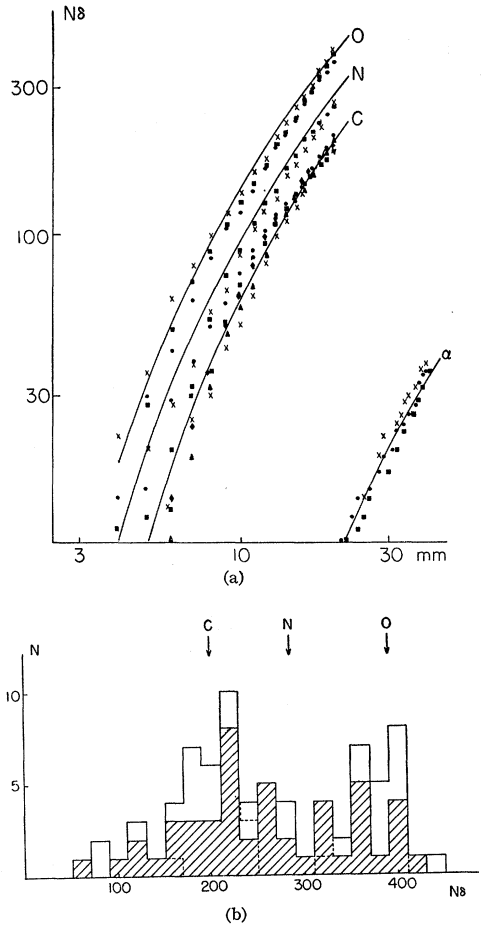

FIG. 4. (a) The calibration of the integrated δ-ray numbers, N_δ, of stopping particles. The N_δ's have been determined with range cutoff of δ-rays at 4.38 μ. The four different symbols used in the figure refer to individual δ-ray countings of four different observers. (b) Charge determination of stopping particles. The unshaded histogram in the figure refers to the work of three different observers and the δ-ray countings on the same track by different observers are counted as different cases. Several tracks, however, have been counted by all three observers and the average taken over the countings of these three observers has been used for each track. This is shown in the shaded histogram.

Though this method, by itself, is a self-consistent method of charge determination, it still seems desirable, if possible, to make additional independent checks on the results, especially on the border line between different charge groups [see Fig. 4(b)].

This has been carried out in the following way. Besides the above mentioned cases of break-ups of $C \rightarrow 3\alpha$ and of $O \rightarrow 4\alpha$ at relativistic energies, we have (1) a track of a Mg nucleus which traversed 8 cm of the stack before it collided with a proton and broke up into five α particles, one deuteron, and one proton; (2) a 9-cm long track of a C nucleus which broke up into three α particles of an energy around 300 Mev; and

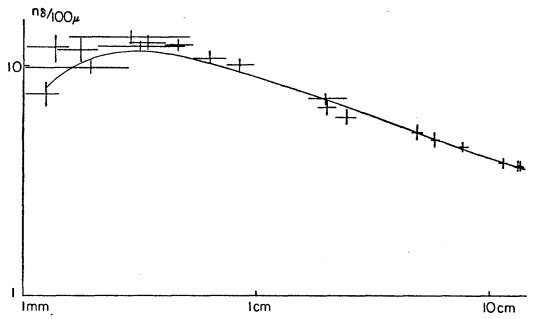

FIG. 5. The calibration curve of the δ-ray density, n_δ, with a range cutoff of δ-rays at 3.70 μ. All results have been converted to carbon. The solid curve is the theoretically expected variation of n_δ with the residual range. The theoretical curve is given by the expression

$$n_\delta = 0.255 \frac{1}{\beta^2}\left\{\frac{m}{E_m}\frac{1-\beta^2}{2\beta^2} - (1-\beta^2)\ln\left(\frac{m}{E_m}\frac{2\beta^2}{1-\beta^2}\right)\right\},$$

with $m/E_m = 10$, the functional form of which has been obtained from the Mott formula for electron scattering on nuclei. For further details, see text.

(3) a track of an O nucleus which broke up into four α particles of energies around 300 Mev. Case (1) is of particular importance here, since except for the deuteron and one of the α particles, all the breakup products as well as the recoil proton stop in the stack and hence their energies are precisely known from their ranges. The energies of the deuteron and α particle which left the stack have been computed by comparing their blob density with those of the neighboring proton and α particles of the same interaction. The energies per nucleon of the five α particles, deuteron, and proton are all nearly the same, 90 to 100 Mev, and differ greatly from the much smaller energy of the recoil proton. Consequently, the assignment of $Z=12$ to the primary particle must be correct. Its energy before interacting is 98 ± 2 Mev per nucleon after a correction due to the binding energy was applied. Hence, we have a track in the stack of known charge, known energy, and known δ-ray density, with a δ-ray range cutoff of 3.30 μ; the δ-rays were counted on various parts of the track. The results are converted to carbon by using the similarity law of δ-ray density mentioned above. They are plotted in Fig. 5.

In the case of the break-up (2), $C \rightarrow 3\alpha$, we cannot make such a precise energy determination. However, because of the long track length of the primary carbon, we can fit the variation with range of the δ-ray density to the curve mentioned above. The results have been found to lie very nicely on the curve of Fig. 5 with respect to both absolute magnitude and variation with range. The energy thus determined turned out to be about 15% higher than that estimated from direct scattering measurement made on the primary carbon track.

The break-up (3) of $O \rightarrow 4\alpha$ has also been incorporated in Fig. 5 by a similar method. In this case, the energy estimate based on scattering measurements of the four α particles has also been found to be 10 to 15% smaller. This might well be due to the fact that the scattering constant we have used[6] is too small for scattering measurements of heavy nuclei or that the elimination of emulsion distortion, which has been done by using two different cell sizes, is insufficient.

The three cases just described give a δ-ray density curve of carbon in the region of residual range from 2 to 14 cm; the points at both ends of this region have been obtained from the track of the Mg nucleus described above. In order to extend the curve to still smaller residual ranges, we selected long stopping tracks, which were analyzed by the above described method and which have been found to fall close to the middle of the carbon peak or the oxygen peak in Fig. 4(b). The two methods give the same charge assignment, and by continuing the δ-ray counting to smaller residual ranges, one can complete the calibration curve for charge determination. The results, all converted to carbon nuclei with the aid of the similarity law, are shown in Fig. 5.

A theoretical curve for the δ-ray intensity could be obtained if one knows both the cutoff energy of the δ-rays and the probability for corresponding δ-rays to be actually counted in the prescribed convention of counting. We, however, regard these two quantities as adjustable parameters and fit the theoretical curve, based on the Mott formula for electron scattering on the nucleus, to the experimental data. The theoretical curve thus obtained is shown in Fig. 5. One can clearly see that the curve passes through the experimental points and it does reproduce the experimental data satisfactorily. Moreover, it has been checked that the theoretical curve actually gives the correct density of δ-rays of the relativistic $C \rightarrow 3\alpha$ as it should. This completes the determination of charge of stopped particles at all energies. The method used here is making use of the range cutoff of δ-rays at a certain known residual range and hence has the advantage that the counting can always be made in a favorable part of the emulsion.

The cases which fell into the borderline regions of

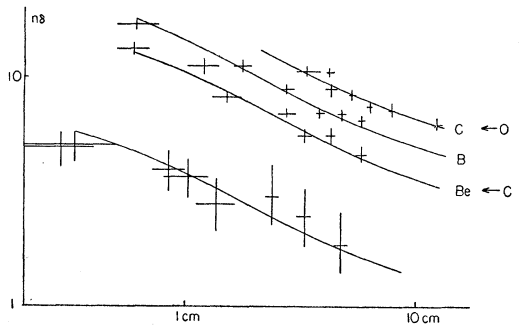

FIG. 6. Calibration curves of the 4-grain δ-ray density *versus* residual range.

[6] E. Pickup and L. Voyvodic, Phys. Rev. **85**, 91 (1952).

neighboring charge peaks in Fig. 4(b) have been analyzed by the above-described method and a good separation between charge groups has been obtained. This completes the analysis of stopping particles.

Before we proceed with the analysis of higher energy tracks, it is convenient to determine a calibration curve for the ordinary 4-grain δ-ray counting. Since we already have a number of stopping tracks of identified charge, a $C \rightarrow 3\alpha$ and an $O \rightarrow 4\alpha$ of known energies, and a relativistic $C \rightarrow 3\alpha$ and a relativistic $O \rightarrow 4\alpha$, it is a simple and straightforward matter to construct this calibration curve. It is, however, to be noted that the similarity law, as represented in Fig. 5, cannot be used here because we have to expect some saturation effect to occur as well as some background contribution. The calibration curves for the 4-grain δ-ray countings are shown in Fig. 6.

Most of the higher energy tracks located by scanning interacted in the stack. The energy estimate in these cases, by means of measuring the opening angles of α particles, for example, cannot be expected to be precise enough for our purposes of obtaining accurate charge and energy spectra in the energy range around 500 Mev per nucleon.

As a consequence, we restrict ourselves to tracks which pass through the stack without interacting and which accordingly at least have a track length of 10 cm available for analysis. These tracks, which we call "through tracks," have been analyzed (1) by the method of the 4-grain δ-ray counting; (2) by the method of counting gaps at the entrance and exit of the track; and (3) by both methods (in some cases) in order to check the consistency, which has actually been verified. Examples of the 4-grain δ-ray countings on these "through" particles are shown in Fig. 7, where each mark represents a track specified by the δ-ray densities at entrance and at exit, both measured 1 cm inside the stack in order to avoid edge effects. Different marks correspond to different observers. The expected variation of the δ-ray densities at exit as a function of the one at entrance has been obtained for each charge from the results plotted in Fig. 6. They are shown by the solid lines in Fig. 7. In order to demonstrate the existance of slow particles among the "through" particles more clearly, in Fig. 8 a histogram is shown with respect to the ratio of the δ-ray densities at each end. One can clearly recognize the slow particles in this histogram.

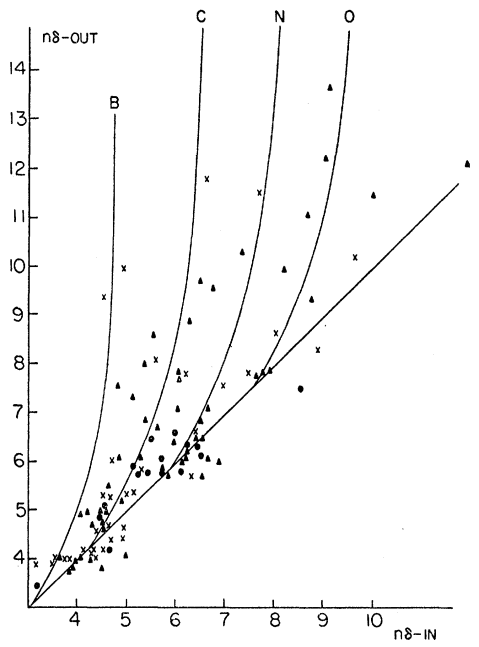

FIG. 7. The results of the 4-grain δ-ray countings on "through" particles are shown in the figure where the variation of n_δ at exit as a function of n_δ at entrance is also given for various charges.

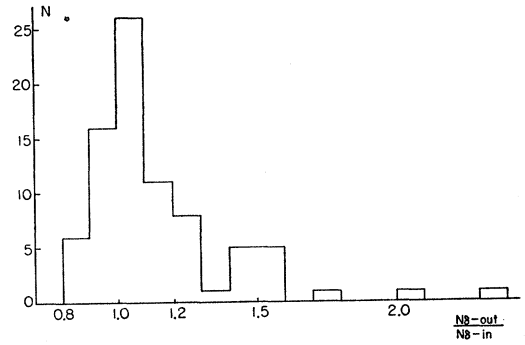

FIG. 8. "Through" particles are classified according to the ratio of n_δ at exit and at entrance, which is in first approximation a function of velocity only. The figure shows the existence of slow particles among the "through" particles.

4. RESULTS

The charge and energy of the heavy nuclei have been determined in the way described in the preceding section. The energy spectrum thus obtained is shown in Fig. 9 for C, N, and O particles. In Fig. 9, the energy has been converted to that at the top of the atmosphere, and a correction has been made for the fact that the heavy nuclei did not interact before stopping or leaving the stack. The point at the highest energy range has been obtained from 72 observed high-energy particles, which have not shown any difference from relativistic particles, by assuming an integral energy spectrum proportional to $(1+E)^{-1.4}$. The numbers in parenthesis in Fig. 9 are the actually observed numbers of particles in the respective energy ranges. One can see a broad maximum in the energy spectrum at energies around 500 to 600 Mev per nucleon. A gradual falling off of the spectrum below the maximum, a feature noticed by the Bristol and Minnesota groups in the energy spectrum of α particles,[3] can also be noticed here. The position of the peak of the α spectrum found by these authors is indicated by an arrow in Fig. 9.

In order to obtain the shape of the spectrum on the low-energy side of the maximum with better statistical accuracy, a supplementary scanning has been carried

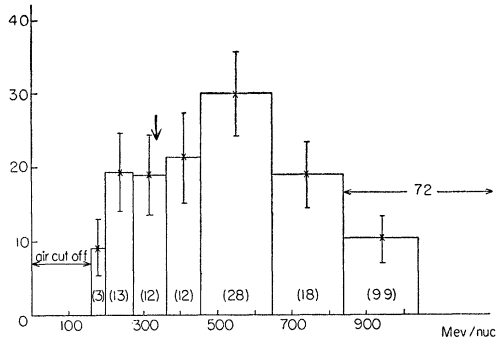

FIG. 9. The energy spectrum of C, N, and O nuclei at the top of the atmosphere. The numbers in parentheses are the numbers of actually observed particles in corresponding energy ranges. For details, see text.

out in which the limit of the projected zenith angle has been changed from the previous value of 20° to 30°. The additional C, N, and O nuclei stopping in the stack have been analyzed by the same methods described in the preceding section. They were added to the ones already used for the energy spectrum of Fig. 9. Figure 10 shows the low-energy part, corresponding to stopping particles only, of the energy spectrum of C, N, and O nuclei with the improved statistics. A gradual decrease toward lower energies is indicated.

The results regarding the relative abundances of C, N, and O nuclei are shown in Table I, where the observed numbers of the respective nuclei are given for two energy ranges. The energies indicated in the table refer to the top of the atmosphere. The results referring to the supplementary scanning for stopping particles are indicated in parenthesis. The relative abundances of C, N, and O nuclei obtained in this work for the energy range between 160 and 840 Mev per nucleon are the same, within the statistical error, as those previously found for higher energies.[2,7]

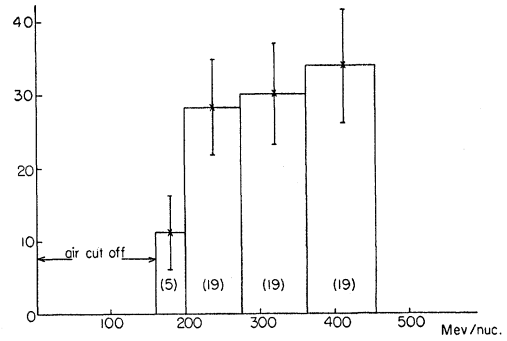

FIG. 10. The lower energy spectrum corresponding to stopping tracks only.

[7] Cester, Debenedetti, Garelli, Quassiati, Tallone, and Vigone, Nuovo cimento **7**, 371 (1958); C. J. Waddington, Phil. Mag. **2**, 1059 (1957); Kaplon, Noon, and Racette, Phys. Rev. **96**, 1408 (1954).

5. DISCUSSION OF RESULTS AND CONCLUSIONS

Low-energy C, N, and O nuclei in the primary cosmic radiation have been identified individually, with respect to both charge and energy, with good precision. As a consequence, the energy spectrum of the C, N, O group has been obtained down to values as low as 160 Mev per nucleon, which is the residual air cutoff for these nuclei in our experiment. At the same time the relative abundances of these nuclei have been determined.

The general characteristics of the energy spectrum of C, N, and O nuclei in the primary cosmic radiation as obtained here does not seem to indicate appreciable differences compared to that found for primary α particles.[3] The position of the maximum particle flux differs somewhat for the two groups, $\sim$550 Mev per nucleon for the C, N, O group and $\sim$300 Mev per nucleon for the α-particle group. This difference in the position of the maximum may possibly be due to the fact that our stack was exposed during the time when the cosmic-ray intensity was recovering to its normal level after the exceptionally large Forbush-type decrease on August 30, 1957. Hence the position of the maximum

TABLE I. The table gives the observed numbers of C, N, and O nuclei in the energy ranges specified in the first row. The numbers in parentheses give the results after the supplementary scanning.

E/nucleon (Mev)	Stopping 160–457	Through 457–840	160–840	$\lesssim$840	Total
C	18 (29)	28	46	35	81
N	10 (14)	10	20	23	43
O	12 (23)	8	20	14	34

in the energy spectrum might have been shifted to a higher energy due to the magnetic storm effect and did not return to normal at the time of our exposure. This point can be clarified by completing the analysis of the energy spectra of the other heavy-nuclei groups, including that of the α particles in the same stack. This work is in progress now.

As has been pointed out for the α-particle group,[3] the existence of a maximum and the gradual decrease below the maximum cannot be due to geomagnetic or atmospheric effects. It is then probable that the energy spectrum of the heavy nuclei had a similar shape before entering the space around the earth.

However, in general, there are two possibilities to consider. First, that the energy spectrum, before entering the solar system, did not exhibit the observed maximum and that it contained very low energy particles down to thermal energy of the source. The existence of a maximum is then to be explained by the effect of magnetic clouds emitted from the sun which prevent the particles of low magnetic rigidity from penetrating into the region around the earth. In this case, we should observe the position of the maximum

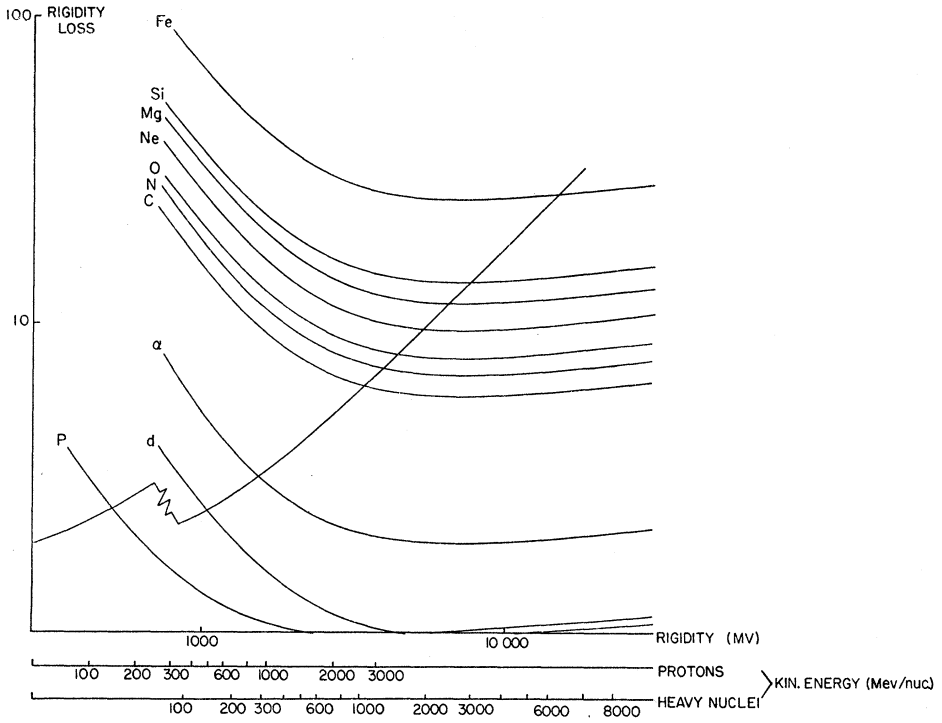

FIG. 11. The figure shows shows the competition between gain and ionization loss in the acceleration process. The rate of rigidity gain is shown in the upward curve crossing the ionization loss curves for various nuclei. The break in the upward curve around 300 Mev per nucleon refers to a normalization procedure used by Fan (reference 9).

at the same magnetic rigidity for the various groups of heavy nuclei, and in general, the spectra should have similar shape, except for some constant factors.

The second possibility is, that even if magnetic clouds do distort the energy spectrum to some extent, the essential features of the spectrum, i.e., the existence of the maximum and the gradual decrease below the maximum, are essentially unchanged before and after entering the solar system. In this case, the shape of the spectrum at very low energies should be closely related to the mechanism of acceleration of cosmic rays.

It is not possible, at present, to decide definitely which of the two possibilities corresponds to the actual situation. However, certain qualitative consequences can be discussed here.

Considering the first possibility, the particles of lowest magnetic rigidity are eliminated due to their long diffusion time through space regions which contain irregular magnetic fields. Hence, if the newly formed magnetic clouds, free of cosmic-ray particles inside, were not supplied with particles by the sun at a rate larger than the diffusion-in of cosmic-ray particles of energies of a few hundred Mev per nucleon, these particles would gradually penetrate into the region of the earth. It can then be expected that the position of the maximum would change with the level of the magnetic activity of the sun.

In this connection, we may recall the results on α particles. The energy spectrum of low-energy α particles has been measured in 1954 and in 1956.[3] Even though there was a large difference in solar activity between these years, the maximum of the energy spectrum remained at the same position within experimental accuracy and the shape of the spectrum did not change appreciably although the over-all intensity of low-energy α particles changed nearly by a factor of two. This implies that the effect of the over-all magnetic activity of the sun, except for solar flares or magnetic storms, does not have a strong effect on the magnetic rigidity spectrum of α particles. Hence it is rather difficult to see how the observed spectrum could have been produced by a solar modulation effect. A spectrum showing a steadily increasing number of particles toward lower energies (no maximum) would also be compatible with a modulation mechanism.

Considering the second possibility, the similarity between the energy spectra of α particles and C, N, and O nuclei has to be explained by a suitable acceleration mechanism. The existence of the maximum might then be due to competition between gain and loss in acceleration processes.[8] An attempt[9] has previously been made along this line of thought for explaining the energy spectrum of the proton component by using Fermi's acceleration mechanism and taking into account ionization loss. However, considering other kinds of particles like heavy nuclei as well the effect of ionization loss introduces difficulties, as has already been pointed out by Fermi in his theory of the origin of cosmic rays.[8] In order to demonstrate the consequences of this effect,

[8] E. Fermi, Phys. Rev. **75**, 1169 (1949); Astrophys. J. **119**, 1 (1954).
[9] C. Y. Fan, Phys. Rev. **101**, 314 (1956).

Fig. 11 has been prepared in which the rigidity loss of protons and heavy nuclei per unit time due to ionization loss is plotted on a relative scale as a function of the magnetic rigidity. The rate of rigidity gain[10] is also given in the same figure. Normalizing at an energy per nucleon of 300 Mev for α particles, it is apparent that we should observe the maximum in the energy spectrum of C, N, and O at around 1.3 Bev per nucleon, which is entirely incompatible with our present results. This would also give rise to difficulties regarding the shape of the proton energy spectrum.[11] We cannot overcome this difficulty by assuming ionization loss in interstellar space after the energy spectra have been formed in some active regions. It would leave the ratio of the two energies, corresponding to the positions of the maxima in the two groups, approximately unchanged.

The experimental results concerning the energy spectra indicate that for α particles and for C, N, and O nuclei, the maximum occurs at roughly the same magnetic rigidity. Therefore, it seems quite natural to consider the possibility that the observed spectra are probably produced by gain and loss processes, both depending chiefly on magnetic rigidity. One of the possible mechanisms is a betatron-type acceleration with scattering-out of particles from regions where the acceleration takes place by magnetic irregularities as gain and loss processes, respectively. The particles, after passing through this stage of preliminary acceleration, may further be accelerated to higher energies by a Fermi-type mechanism in interstellar space. However, one should bear in mind that the first possibility, to explain the spectrum by the effect of solar activity, is not completely excluded, though it seems rather unlikely, in view of the above mentioned considerations.

Regarding the relative abundances of C, N, and O nuclei in the primary cosmic radiation, inspection of Table I shows that the relative abundances of these nuclei do not seem to change with energy.[2,7] This would imply that the same type of ion source is responsible for the origin of both high- and low-energy cosmic rays.

The observed relative abundances further indicate that carbon is more abundant than nitrogen or oxygen at low energies. This relatively large abundance of carbon suggests that the ion source of cosmic rays is not in an equilibrium state with respect to the carbon-nitrogen cycle. Hence, the relative abundances of C, N, and O are probably due to a transient state in the evolutionary life of certain stars.[12]

Studies of the relative abundances of the other nuclei, especially F and Ne, should yield additional information concerning the ion source of the cosmic radiation.

ACKNOWLEDGMENTS

We wish to thank Professor G. Burbidge and Professor S. Hayakawa for stimulating discussions. Our thanks are also due to G. Schultz, L. Henry, L. Loetscher, and B. Price of the University of Chicago, and K. Murakami and T. Yoshizawa of the Institute for Nuclear Study, University of Tokyo, for their aid both in scanning and analysis work.

[10] As an example, a rigidity gain which is proportional to $\gamma=[(Z_R/M)^2+1]^{\frac{1}{2}}$ is plotted in the figure. The Fermi acceleration gives the same rigidity dependence in the relativistic limit.

[11] J. A. Van Allen and J. R. Winckler, Phys. Rev. **106**, 1072 (1957); M. A. Pomerantz and G. W. McClure, Phys. Rev. **86**, 536 (1952).

[12] Burbidge, Burbidge, Fowler, and Hoyle, Revs. Modern Phys. **29**, 547 (1957).